

Finite element analysis of deep beams on nonlinear elastic foundations

A. A. Al- Azzawi¹, A. H. Mahdy² and O. Sh. Farhan³

¹Nahrian University, Baghdad, Iraq
dr_adel_azzawi@yahoo.com

²Nahrian University, Baghdad, Iraq
aula84@yahoo.com

³Nahrian University, Baghdad, Iraq
ommar-shamal2006@yahoo.com

Abstract

This research deals with the nonlinear material and geometric behaviors of reinforced concrete deep beams resting on linear or nonlinear Winkler foundation. The finite elements through ANSYS (Release-11, 2007) computer software are used. The reinforced concrete deep beam is modeled using (SOLID 65) 8 node brick element and the soil is modeled using linear spring (COMBIN 14) element or nonlinear spring (COMBIN39) element.

The results obtained from the present study are compared with available analytical or experimental results. Good agreement is obtained with available results which also indicate the efficiency of the finite element method used to model the problem. The difference in maximum deflection between large and small deflections theory is found to be small. The maximum stress is increased when the beam is resting on nonlinear Winkler foundation because of reduced foundation stiffness.

Several important parameters are incorporated in the analysis - namely the vertical subgrade reaction, mesh size, and compressive strength of concrete - to study their effects on the beam behavior. The results demonstrate that the difference in maximum deflection between the linear and nonlinear model of soil is about (2.5%).

Key words: Deep beams, finite elements, nonlinear elastic foundations

1. Introduction

Beams are one dimensional structural element that can sustain transverse loads by the development of bending, twisting and transverse shearing resistances in the transverse sections of the beam. Mainly, two theories could be used for basic formulation of flexural beam models. In the case of a thin beam, the model is based on the classical theory (Euler-Bernoulli). This theory is based on the fundamental assumptions that the cross-sections of the beam remain plane and normal to the axis of bending, after loading it also implies that the strains and rotations of the beam are small compared to the beam depth. In the other case of a deep beam, the model is based on Timoshenko's theory. This theory considers the effect of transverse shearing deformations. Thus, the cross sections of the beam remain plane but not necessarily

normal to the axis of bending. Deep beams are structural elements having a large (depth to span) ratio in which a significant amount of the load is transferred to the supports by a compression thrust joining the load and the reaction. As a result, the strain distribution is no longer considered linear, and the shear deformations become significant when compared to pure flexure. Beams having a ratio of span to depth 5 or less are called deep beams.

Reinforced concrete structures or deep beams are usually analyzed using first order linear load deflection relationship and both strains and displacements developed in the structure are assumed to be small. This means that geometric nonlinearities are not taken into account; therefore the expected behavior of the member differs from the real behavior leading to approximate solutions. The percentage difference in results if geometric nonlinearity included is unknown. It is known that plain concrete has low tensile strength, limited ductility and little resistance to crack propagation. Flaws or micro-cracks develop in the concrete during its manufacture and even before any load is applied. In compression, these micro-cracks propagate up to about one-third of the ultimate strength. In tension, they lead to brittle failure at about one-tenth of the compressive strength

Jamal (1997) utilized the large displacement analysis procedure for the beam-column element with gusset plates at its ends. A new formula for stability and bowing functions was derived. A developed local tangent stiffness matrix was obtained and used in the solutions of several examples.

Al-Hachmi (1997) presented a theoretical analysis for predicting the large displacement elastic stability analysis of plane and space structures subjected to general static loading. The beam-column theory was used in the analysis, taking into accounts both bowing and axial force effects. The general equations of fixed end moments of a beam subjected to lateral loads were also derived. The work employed the analysis to study the behavior of beams with elastic foundations, piles driven into soil, and large displacements of submarine pipelines.

Chen (1998) presented a new numerical approach for solving the problem of beams resting on an elastic foundation. The approach used the differential quadrature (DQ) to discretize the governing differential equations defined on all elements, the transition conditions defined on the inter-element boundaries of two adjacent elements, and the boundary conditions of the beam. By assembling all the discrete relation equations, a global linear algebraic system can be obtained. Numerical results of the solutions of beams resting on elastic foundations obtained by the *DQEM* were presented.

Yin (2000-a) suggested a method for obtaining closed-form solutions for a reinforced concrete Timoshenko beam resting on an elastic foundation subjected to different pressure loading. A particular solution was obtained for uniform pressure loading at any location of the beam. This solution can be used to calculate settlement, rotation, bending moment and shear force of the beam.

Yin (2000-b) derived the governing ordinary differential equations for a reinforced Timoshenko beam on an elastic foundation. An analytical solution was obtained for a point load on an infinite Timoshenko beam on an elastic foundation. Special attention was drawn to the location, tension and shear stiffness of reinforcement and its influence on settlement or deflection of the beam and reinforcement tension force. A finite element model was established for the same infinite beam problem.

Onu (2000) derived a formulation leading to an explicit free-of meshing stiffness matrix for a beam finite element foundation model. The shear deformation contribution was considered and the formulation was based on exact solution of the governing differential equation. Two numerical examples were presented. The first one, a short beam on an elastic foundation was analyzed to validate the shear stiffness matrix. The second example examined a structure-

foundation interaction problem of a seven-story building supported by a foundation beam on a two-parameter foundation model.

Aristizabal-Ochoa (2001) developed, in a simplified manner, a nonlinear large deflection-small strain analysis of a slender beam-column of symmetrical cross section with semi rigid connections under end loads (conservative and non conservative), including the effects of axial load eccentricities and out-of-plumpness. Timoshenko's stability functions were utilized in the proposed method which, although approximate, can be used in the stability and nonlinear large deflection small strain elastic analyses of beam-columns with rigid, semi rigid and simple connections.

Mahmoud (2001) used the rectangular isotropic eight node element for the representation of the concrete, while the steel was represented by a layer. He considered the effect of nonlinear behavior, bond slipping and the shear transfers of the concrete after the cracks appeared. The steel was considered as one dimensional elastic-plastic and a computer program was used to study the nonlinear behavior of structures and the result for the deflection and the stress and strain for different structures were obtained.

Guo and Weitsman (2002) made an analytical method, accompanied by a numerical scheme, to evaluate the response of beams on non uniform elastic formulation, where the foundation modulus is $K_z = K_z(x)$. The method employed Green's foundation formulation, which results in a system of nonsingular integral equations for the distributed reaction $p(x)$. These equations can be discretized in a straightforward manner to yield a system of linear algebraic equations that can be solved by elementary numerical techniques.

Lazem (2003) presented a theoretical analysis for large displacement elastic stability of in-plane structures where some members were embedded into or resting on elastic foundations. The analysis was based on Eulerian formulation, which was developed initially for elastic structures and was extended to include soil-structure interaction. Local member force-displacement relationship is based on beam-column approach.

Al-Azzawi and Al-Ani (2004) studied the linear elastic behavior of thin or shallow beams on Winkler foundations with both normal and tangential frictional resistances. The finite difference method was used to solve the governing differential equations and good results were obtained with the exact solutions for different load cases and boundary conditions.

Al-Musawi (2005) studied the linear elastic behavior of beams resting on elastic foundations with both compressional and tangential resistances. The finite element method in Cartesian coordinates is formulated using different types of one, two and three dimensional isoparametric elements to compare and check the accuracy of the solutions. A computer program coded in **fortran_77** for the analysis of beams on elastic foundations was developed in his study.

Al-Shraify (2005) presented a three-dimensional nonlinear finite element model suitable for the analysis of reinforced concrete members. Concrete was modeled using 20-node isoparametric quadratic elements, while the reinforcing bars were modeled as axial members embedded within the concrete elements. The nonlinear equations of equilibrium have been solved using an incremental-iterative technique based on the modified Raphson methods.

Al-Talaqany (2007) studied the geometric nonlinear behavior of beams resting on Winkler foundation. Timoshenko's deep beam theory is extended to include the effect of large deflection theory. In the finite element method, the element SHELL 43 incorporated in ANSYS 5.4 was used. The finite difference method was also used to solve the problem of thin and deep beams and the obtained results were compared with the finite element method results (ANSYS program) to check the accuracy of the developed analysis. An incremental load approach with

Newton-Raphson iteration computational technique was used for solving the nonlinear sets of node equilibrium equations in the finite difference method.

Andrejev (2008) made a survey of evolution of the theory about the constructions, placed on elastic foundation. Methods of computation of the reinforced beams, placed on elastic foundation, with accepted assumptions were analyzed. Application of the solutions, pertaining to beams placed on elastic foundations, towards the construction elements, meant for the other assignments were considered.

The present study deals with the nonlinear material and geometric behaviors of reinforced concrete deep beams resting on linear or nonlinear Winkler foundation. The finite elements through ANSYS (Release-11, 2007) computer software are used in this study. The reinforced concrete deep beam is molded using (SOLID 65) 8 node brick element and the soil is molded using linear spring (COMBIN 14) element or using nonlinear spring (COMBIN39) element. The simplest soil model is used in the present study because the main task is to study the reinforced concrete deep beam behavior rather than the soil or interface behavior. The interface elements between concrete and soil or steel reinforcement and concrete will not included in the present study.

2. Material modeling

2.1 Concrete

2.1.1 Modeling of concrete in compression

The behavior of concrete in compression can be simulated in ANSYS-11 by an elastoplastic work hardening model followed by a perfectly plastic response, which is terminated at the onset of crushing. The model used for compression is expressed in terms of yield criterion, a hardening rule and a flow rule.

2.1.1.1 Yield criterion

The material is assumed to behave elastically until it reaches the yield limit. For isotropic materials, the initial yield criterion should be independent of the orientation of the coordinate system in which the stress state is defined and therefore, it should be a function of the stress invariants only (Chen 1982). The yield criterion adopted in ANSYS-11 is the von-Mises criterion. It can be expressed as:

$$f(\{\sigma\}) = \left[\frac{3}{2} \{s\}^T [M] \{s\} \right]^{1/2} = \sigma_o \quad (1)$$

where,

$\{s\}$ is the deviatoric stress:

$$\{s\} = \{\sigma\} - \sigma_m [1 \ 1 \ 1 \ 0 \ 0 \ 0]^T \quad (2)$$

where,

$\{\sigma\}$ is the stress vector.

σ_m is the mean stress:

$$\sigma_m = \frac{1}{3}(\sigma_x + \sigma_y + \sigma_z) \tag{3}$$

and σ_o is the equivalent effective stress.

2.1.1.2 Hardening rule

The hardening rule is required to define the expansion of the loading surfaces during plastic deformation. To describe the growth of the subsequent loading surfaces for strain or work-hardening materials, many hardening rules are adopted to simulate concrete behavior. The hardening rule adopted by ANSYS-11 assumes that the yield surface expands uniformly without distortion as plastic deformation occurs as shown in figure 1 (Chen 1982).

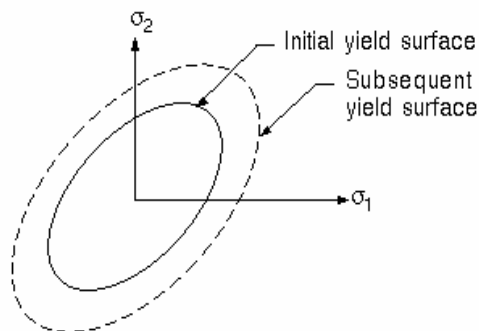


Fig. 1. Isotropic work hardening.

Therefore, the subsequent loading surfaces may be written as:

$$f(\{\sigma\}) = \left[\frac{3}{2} \{s\}^T [M] \{s\} \right]^{1/2} = \bar{\sigma} \tag{4}$$

where, the effective stress or equivalent uniaxial stress $\bar{\sigma}$ represents the stress level at which further plastic deformation will occur. In the present work, the effective stress $\bar{\sigma}$ can be determined directly from the equivalent plastic strain $\hat{\epsilon}_n^{pl}$ given in the following expression:

$$\bar{\sigma} = \sigma_y + \frac{E_c E_T}{E_c - E_T} \hat{\epsilon}_n^{pl} \tag{5}$$

where,

E_c = modulus of elasticity.

E_T = tangent modulus from multilinear uniaxial stress-strain curve, [Fig. 2].

$$\hat{\epsilon}_n^{pl} = \hat{\epsilon}_{n-1}^{pl} + \Delta \hat{\epsilon}^{pl} \tag{6}$$

where,

$\hat{\epsilon}_n^{pl}$ = equivalent plastic strain for this time point, and

$\hat{\varepsilon}_{n-1}^{pl}$ = equivalent plastic strain from the previous time point.

If there is no plastic strain ($\hat{\varepsilon}^{pl} = 0$), then $\bar{\sigma}$ is equal to the yield stress. The equivalent uniaxial stress $\bar{\sigma}$ only has meaning during the initial, monotonically increasing portion of the load history. If the loads were to be reversed after plastic loading, the stresses would fall below yield but $\bar{\sigma}$ would register above yield (since $\hat{\varepsilon}^{pl} \neq 0$).

In order to define the expansion of the current loading surface, the incremental theory of plasticity implies a relationship between the accumulated (effective) plastic strain ($\hat{\varepsilon}_n^{pl}$) and effective (equivalent) stress ($\bar{\sigma}$) to extrapolate the results of a uniaxial test to a multiaxial situation.

In the present model, a multilinear stress-strain curve is used for the uniaxial stress-strain relationship beyond the limit of elasticity, $0.3f'_c$. This parabolic curve represents the work-hardening stage of behavior. When the peak compressive stress is reached, a perfectly plastic response is assumed to occur. Figure (2) shows the equivalent uniaxial stress-strain curve adopted by ANSYS-11 at various stages of loading.

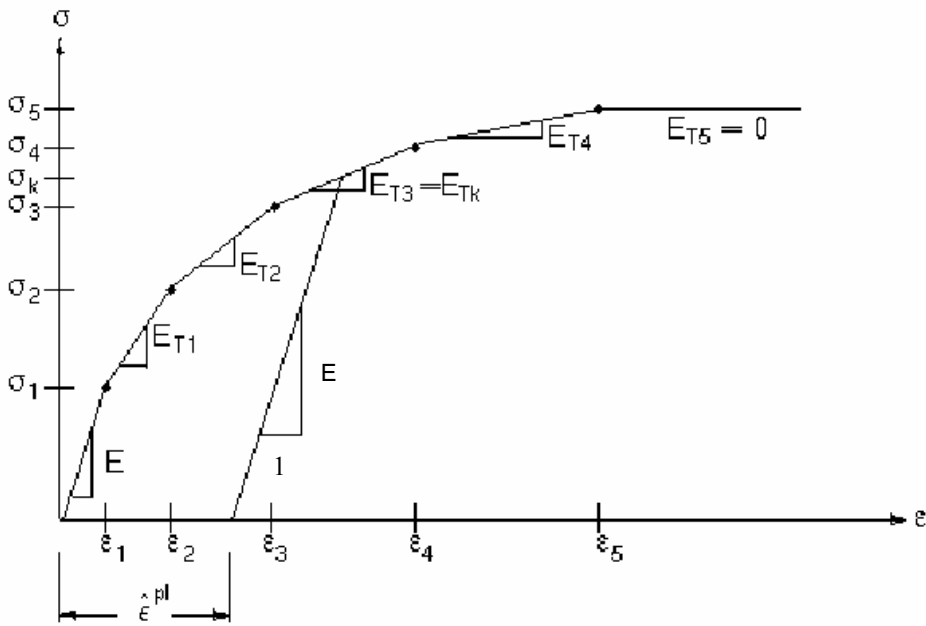


Fig. 2. Multilinear stress-strain curve for concrete adopted in the analysis.

2.1.1.3 Flow rule

To construct the stress-strain relationship in the plastic range, an associated flow rule is usually employed. This means that the plastic deformation rate vector will be assumed normal to the yield surface. The plastic strain increment can be determined for a given stress increment as (Chen (1982):

$$d\{\varepsilon_p\} = \lambda \frac{\partial f(\{\sigma\})}{\partial \{\sigma\}} \quad (7)$$

where, λ is the hardening or the loading parameter which determines the size of the plastic strain increment and $\partial f\{\sigma\}/\partial\{\sigma\}$ defines the direction of the plastic strain increment vector $d\{\varepsilon_p\}$ as normal to the current loading surface.

2.1.2 Behavior of concrete in tension

Linear elastic model prior to cracking is usually used to simulate the behavior of concrete in tension. In general, the cracking criterion of concrete is expressed in terms of principal tensile stresses or strains. In the ANSYS-11, the onset of cracking is controlled by a maximum principal stress criterion. A smeared crack model with fixed orthogonal cracks is adopted to represent the fractured concrete (Chen 1982).

The tensile stresses normal to the cracked plane are gradually released, and are usually represented by an average stress-strain curve. To obtain such a relationship, either the tension-stiffening or strain-softening concepts may be used. In the present work, the tension-stiffening concept is adopted. Since the cracked concrete can still initially carry some tensile stresses in the direction normal to the crack, the tension-stiffening effect is considered. This has been achieved in ANSYS-11 by assuming gradual release of the concrete stress component normal to the cracked plane. In the present work, the normal stress that is carried by cracked concrete can be obtained from figure 3.

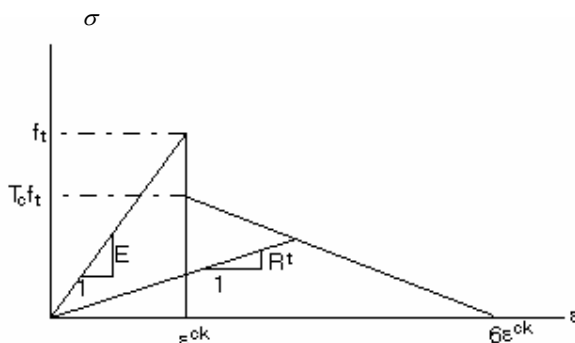


Fig. 3. Post cracking model for concrete.

where, ε_{cr} is the cracking strain, f_t is the uniaxial tensile cracking stress, T_c is the multiplier for amount of tensile stress (default in ANSYS11 = 0.6).

Three different approaches for crack modeling have been employed in the analytical studies of concrete structures using the numerical technique of the finite element method. These are smeared cracking modeling as shown in figure 4, discrete cracking modeling as shown in figure 5, and fracture mechanics modeling (Chen 1982). For (ANSYS-11) computer program, crack modeling of concrete depends on smeared cracks.

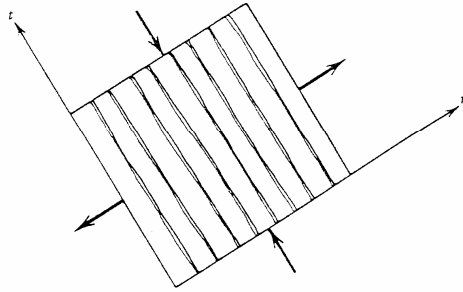


Fig. 4. Representation of a single crack in the smeared crack modeling approach (Chen 1982).

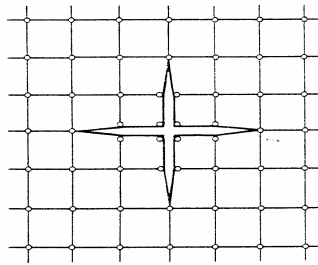


Fig. 5. Two dimensional cracking representation in discrete crack modeling approach (Chen 1982).

2.1.3 Crushing modeling

If the material at an integration point fails in uniaxial, biaxial or triaxial compression, the material is assumed to crush at that point. Under this condition, the material strength at the considered integration point is assumed to have degraded to an extent such that its contribution to the stiffness of an element in question can be ignored (ANSYS-11).

2.1.4 Multiaxial behavior of concrete

The response of concrete under triaxial compressive stresses, will exhibit strength, which increases with the confining pressure. Under very high confining stresses, extremely high strengths have been recorded. Experimental studies indicate that the three dimensional failure envelope is a function of the three principal stresses. Figure 6 shows a schematic failure surface of concrete in three dimensional stress space. The failure envelope is smooth, convex and its deviatoric sections (planes perpendicular to the hydrostatic axis, line of $\sigma_1 = \sigma_2 = \sigma_3$) become more circular in shape for increasing hydrostatic pressures. For smaller hydrostatic pressures, these cross sections are convex and non-circular (Chen 1982).

The model to be used is capable of predicting failure for concrete materials. Both cracking and crushing types of failure model are accounted for. The two input strength parameters (i.e. ultimate uniaxial tensile and compressive strengths) are needed to define a failure surface of concrete. Consequently, a criterion for failure of concrete due to multiaxial stress states can be calculated. The limiting tensile stress required to define the onset of cracking can be calculated for states of triaxial tensile stress and for combinations of tension and compression principal

stresses. The stress function adopted in the present work has been used by William and Warnke. Both the function of stress and the failure surface are expressed in terms of principal stresses denoted as σ_1 , σ_2 and σ_3

where, $\sigma_1 = \max(\sigma_x, \sigma_y, \sigma_z)$

$$\sigma_3 = \min(\sigma_x, \sigma_y, \sigma_z)$$

and if $\sigma_1 \geq \sigma_2 \geq \sigma_3$, the failure of concrete is categorized into four domains:

1. $0 \geq \sigma_1 \geq \sigma_2 \geq \sigma_3$ (compression- compression- compression).
2. $\sigma_1 \geq 0 \geq \sigma_2 \geq \sigma_3$ (tension- compression- compression).
3. $\sigma_1 \geq \sigma_2 \geq 0 \geq \sigma_3$ (tension- tension- compression).
4. $\sigma_1 \geq \sigma_2 \geq \sigma_3 \geq 0$ (tension- tension- tension).

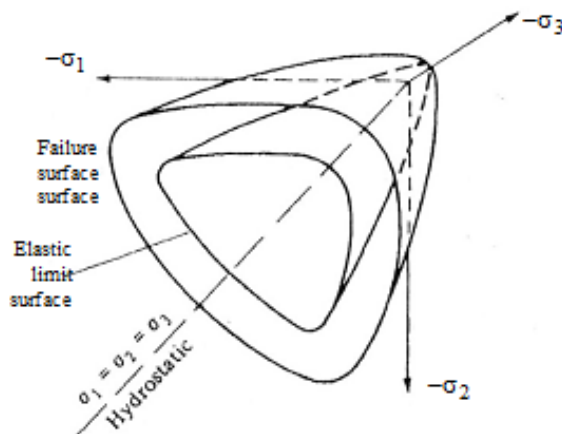


Fig. 6. Schematic representation of the elastic limit and failure surface of concrete in the three dimensional principal stresses..

2.2 Reinforcement steel modeling

The mechanical properties of steel in compression are well known and understood. Steel is a homogeneous material and the stress-strain curves for steel are generally assumed to be identical in tension and compression, and it can generally be assumed to be capable of transmitting axial force only. Steel bars in reinforced concrete members are normally long and relatively slender and therefore they can be generally assumed to be capable of transmitting axial forces only. Steel fabric reinforcement is normally produced from cold formed steel wire (grade 460) with a regular mesh arrangement. During cold forming process, steel may be stressed beyond its yield stress into strain hardening (Chen 1982). In the present study, the uniaxial stress-strain behavior of reinforcement is simulated by an elastic-linear work hardening model as shown in figure 7.

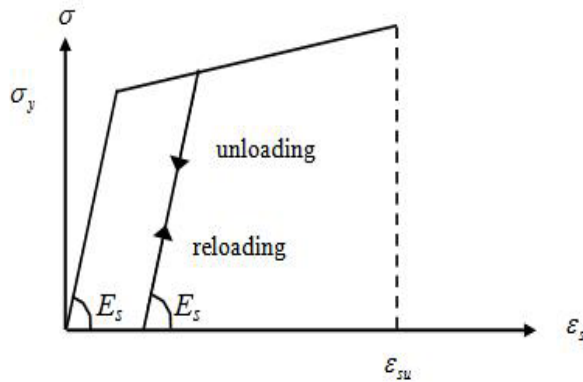


Fig. 7. Stress strain relationship of steel bar.

2.3 Elastic models of soil behavior

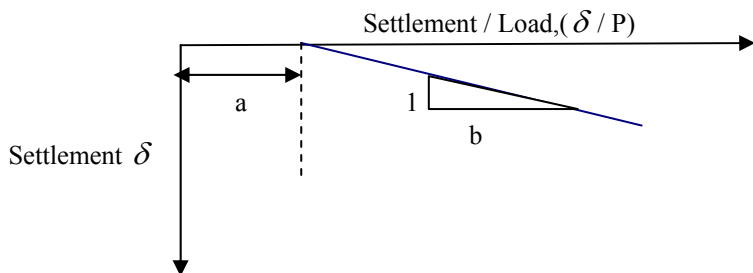
In order to perform nonlinear analysis of soil, however, it is necessary to be able to describe the load-deflection behavior of soil in quantitative terms, and to develop techniques for incorporating this behavior in the analysis. The modulus of subgrade reaction gives the relationship between the soil pressure and the resulting deflection. Soil configuration can be presented by using two kinds of moduli along the foundation length, the normal and tangential. The normal modulus (K_z) is conventional subgrade reaction modulus. The tangential modulus (K_t) is the amount of skin-friction required to mobilize a unit axial displacement in the soil around the soil-structure interaction element.

Since the behavior of the soil under compressive loading is nonlinear as verified by the results of plate-load test and considering the load settlement curve a plate-load test in the field, the beam element resting on soil can approximate the response by using the two-constant hyperbolic stress-strain equation

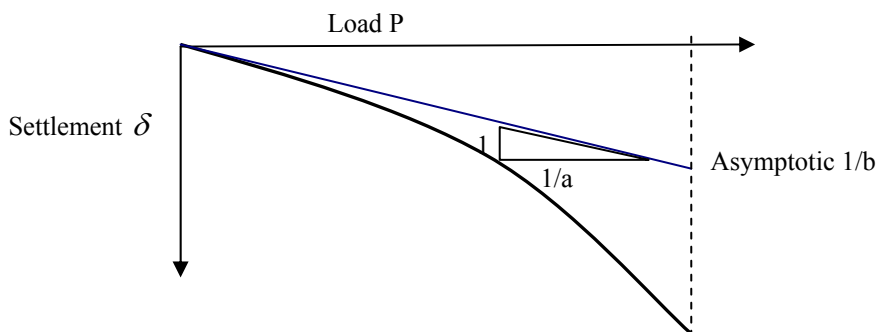
$$P = \delta / (a + b \delta) \quad (8)$$

$$K_z = a / (a + b \delta)^2 \quad (9)$$

where, P is the lateral load on beam element which is concentrated at the node, δ is the lateral displacement of the node and K_z is the normal subgrade reaction of the soil, a and b are the physical parameters required for the hyperbolic equation which can be obtained from the load-settlement curve of the plate-load test. As shown in figure 8, " a " is the reciprocal of the initial tangent to the load-settlement curve of the plate-load test, and " b " is the reciprocal of the asymptotic value of load P at which the plate will continue to penetrate into the soil without any increment of the load applied (Hateam 2001). This model has been used in the present study.



a-Hyperbolic load-settlement curve of plate-load test .



b-Transformed hyperbolic load settlement curve .

Fig. 8. Plot of load settlement.

3. Finite element analysis

3.1 Reinforced concrete beam

In the current study, three dimensional isoparametric solid elements (SOLID65) are used to model the reinforced concrete. The element is defined by eight nodes having three degrees of freedom at each node: translations in the nodal x , y and z directions. Up to three rebar specifications may be defined. The solid cracks in tension and crushes in compression are studied. The solid capability of the element may be used to model the concrete while the rebar capability is available for modeling the reinforcement, [Fig. 9]. The reinforcement, which also incorporates plasticity, is assumed to be smeared throughout the element. Directional orientation is accomplished by user specified angles.

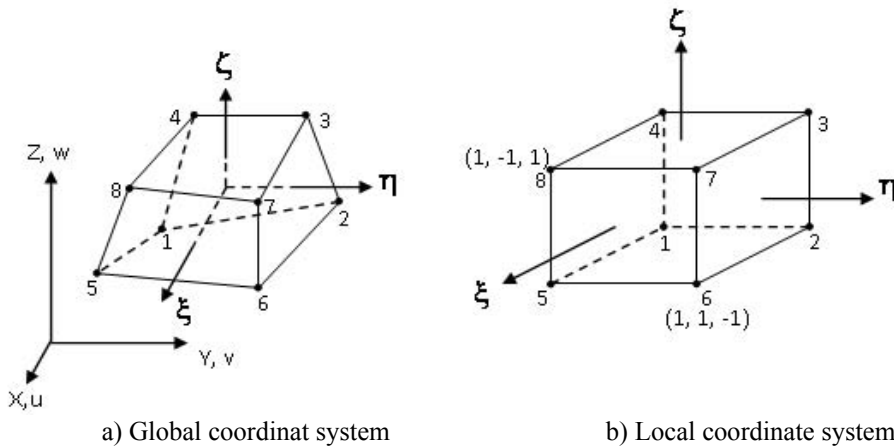


Fig. 9. 8-node 3-D reinforced concrete solid element.

Analysis of RC structures using the finite element method requires a simple, yet accurate way of representing the reinforcement. Three alternative representations have been usually used to simulate the reinforcement, which are:

- I) Embedded reinforcement.
- II) Smeared reinforcement.
- III) Discrete reinforcement.

The embedded representation assumes that the reinforcing bar as an axial member is built into the isoparametric element which displacements are consistent with those of the element. The bars are restricted to lie parallel to the local coordinate axes of the basic element and perfect bond must be assumed between concrete and the reinforcement.

For the smeared representation, the steel bars are assumed to be distributed into an equivalent layer within the concrete with axial properties in the direction of the bars only. A composite concrete – reinforcement constitutive relationship is used in this case and perfect bond is assumed between concrete and steel bars.

A discrete representation of the reinforcement using one – dimensional element is the most widely used. For two dimensional analysis axial bar members with two degrees of freedom at each node are usually employed. A one dimensional flexural element with three degrees of freedom per node has also been adopted. A significant advantage of the discrete representation, in addition to its simplicity can account for possible displacement of reinforcement with respect to the surrounding concrete. Their disadvantages are to restrict the mesh and increase the total number of elements (Collins and Mitchell 1991). In the present study, the smeared and discrete representation are used. LINK8 which has been used to model the reinforcement is a bar (or truss) element which may be used in a variety of engineering applications. This 3-D spar element is a uniaxial tension-compression element with three degrees of freedom at each node. In translation in the nodal x , y , and z directions, as in a pin-jointed structure, no bending of the element is considered. This element is used in the present study to simulate the behavior of reinforcing bars which work as stirrups in resisting the vertical shear in concrete and main steel reinforcement in resisting the flexural stresses. The geometry, node locations, and the coordinate system for the element are shown in figure 10.

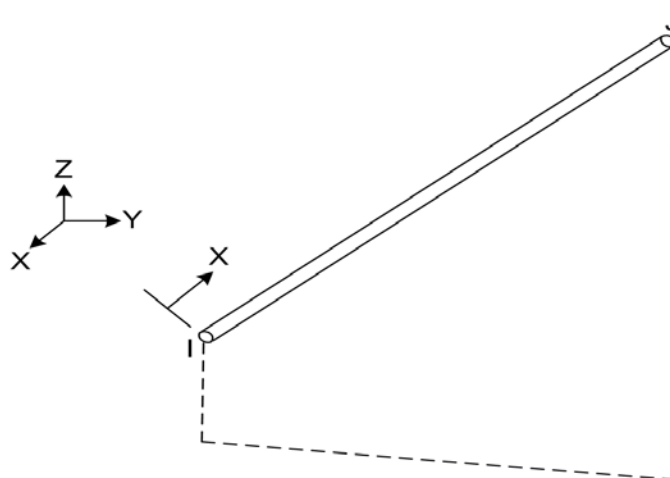


Fig. 10. LINK8 – 3-D spar.

3.2 Elastic foundations

The models of soil behavior for which the relationship between the applied forces and resulting displacements are given by linear or nonlinear functions are considered in this study.

The stress-strain of any type of soil depends on a number of different factors including density, water content, structure, drainage conditions, strain condition (i.e. plane strain, triaxial), duration of loading, stress history, and confining pressure.

The idealized model of soil media as proposed by Winkler in 1867 assumes that normal pressure p of the soil medium (soil reaction) at any point on the surface is directly proportional to the deflection w at that point and is independent of deflections occurring at other locations. Winkler idealization of the soil medium consists of a system of independent closely spaced spring elements with spring constant K_z (per unit deflection). One important feature of this soil model is that the z -displacement occurs immediately under the loaded area and outside this region the displacement is zero.

Since the surface deflection in Winkler model is limited to the loading region, thus this model is restricted in applicability to soil media which possess very slight amount of cohesion for transmissibility of applied forces. It is a common experience that, in the case of soil media, surface deflections will occur not only immediately under the loaded region but also in certain limited zones neighboring the loaded region. In general, the application of the continuum theory of classical elasticity to soil-foundation interaction presents a complex mathematical problem (Al-Musawi 2005).

3.2.1 Linear spring element

The (COMBIN14) element or the longitudinal element spring-damper option is a uniaxial tension-compression element with up to three degrees of freedom at each node: translations in the nodal x , y , and z directions. No bending or torsion is considered. If damping is neglected the spring element will simply represent the linear Winkler model of one parameter K_z which is the simple model to represent soil [Fig.11]

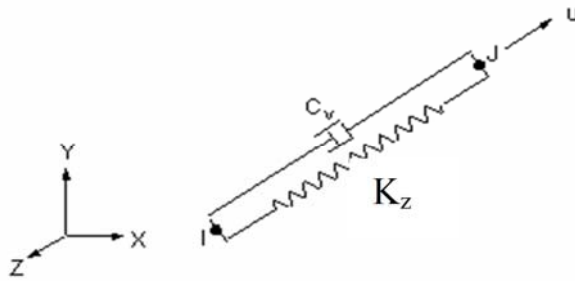


Fig. 11. Linear spring element.

$$[K^e] = K_z \begin{bmatrix} 1 & -1 \\ -1 & 1 \end{bmatrix} \quad (10)$$

$$[C^e] = C_v \begin{bmatrix} 1 & -1 \\ -1 & 1 \end{bmatrix} \quad (11)$$

and $C_v = C_{v1} + C_{v2} |v|$.

where, K_z is the spring stiffness, C_{v1} is the constant damping coefficient, C_{v2} is the linear damping coefficient and v is the relative velocity between nodes computed from the nodal Newmark velocities.

3.2.2 Nonlinear spring element

The (COMBIN39) element is a unidirectional spring element with nonlinear generalized force-deflection capability. The element has a longitudinal capability (uniaxial tension-compression element) with up to three degrees of freedom at each node: translations in the nodal x , y and z directions. No bending or torsion is considered. The element is defined by two nodes and is used to resist slip [Fig. 12]. COMBIN39 spring element will simply represent the nonlinear Winkler model of one parameter K_z with different values obtained from the slope of load settlement curve which is the improved model of COMBIN14.

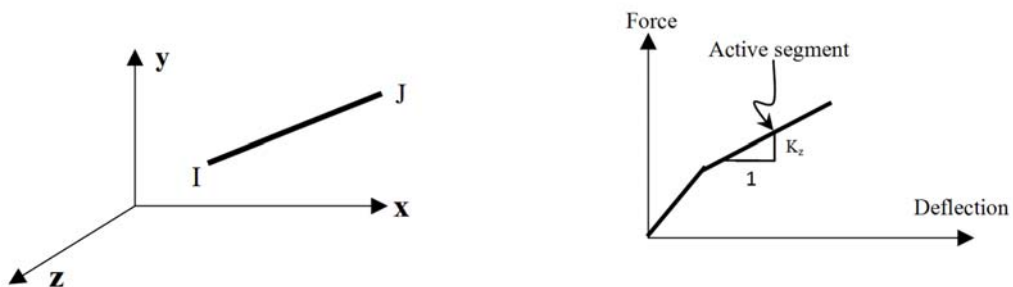


Fig. 12. Nonlinear spring element

The stiffness matrix of the element is given by:

$$[K^e] = K_z \begin{bmatrix} 1 & -1 \\ -1 & 1 \end{bmatrix} \quad (12)$$

where, K_z is the slope of active segment of the force-deflection curve of this element, [Fig. 12].

4. Applications for testing the models

The numerical results obtained from the finite element analysis have been compared with available analytical and numerical results to check the accuracy of the method used in this study. The case studies include the geometric and material nonlinear behavior of beams resting on (Winkler type) elastic foundations.

4.1 Uniformly loaded simply supported deep beam resting on Winkler foundation

A beam of ($E=25 \times 10^6$ kN/m², $\nu=0.15$) and having a length of (2.0m), width ($b=0.4$ m), depth ($h=0.8$ m) and subjected to a uniformly distributed load ($q=62.5$ kN/m²), is considered as shown in figure 13. The beam is resting on Winkler foundation with coefficient ($K_z=10000$ kN/m³). This problem was solved by (Al-Talaqany, 2007) by using the finite difference method. In the present study, this problem is solved by using the finite element method with ANSYS program. The beam is modeled using 144 brick elements (SOLID65) with 8 node and the foundation is represented by 40 linear spring elements (COMBIN14) as shown in figure 14. The results of deflections, normal, and shear stresses are plotted with the results of Al-Talaqany (2007) as shown in figures 15 to 18. The figure 16 shows acceptable agreement for deflections. The percentage of difference between the maximum deflections for Al-Talaqany, (2007) solution and the present study is (10%). There is small difference between large and small deflection analyses by about (0.0012%) because of adding the stiffness of foundation.

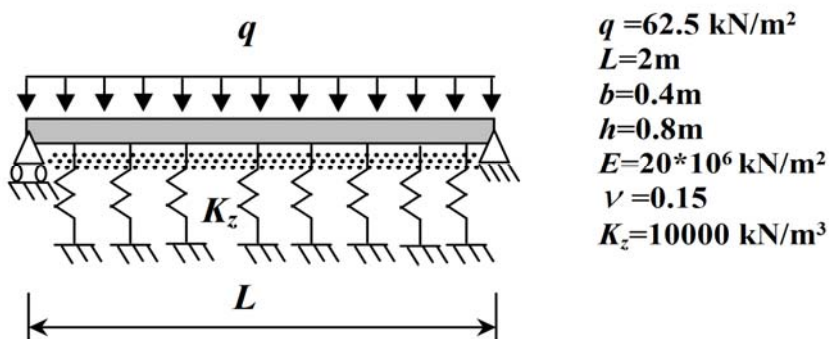


Fig. 13. Uniformly loaded simply supported deep beam resting on Winkler foundation.

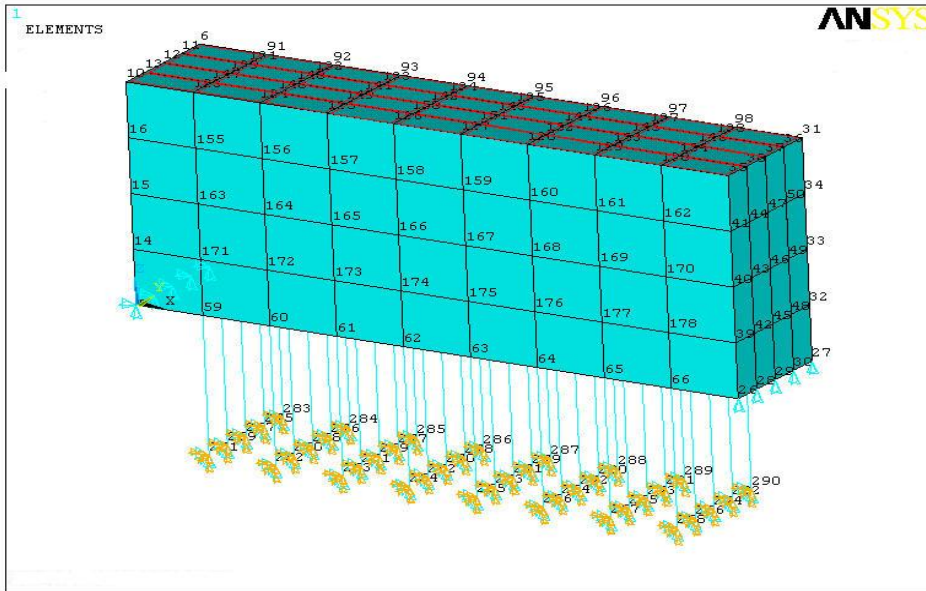


Fig. 14. Finite element mesh of uniformly loaded simply supported deep beam resting on Winkler foundation.

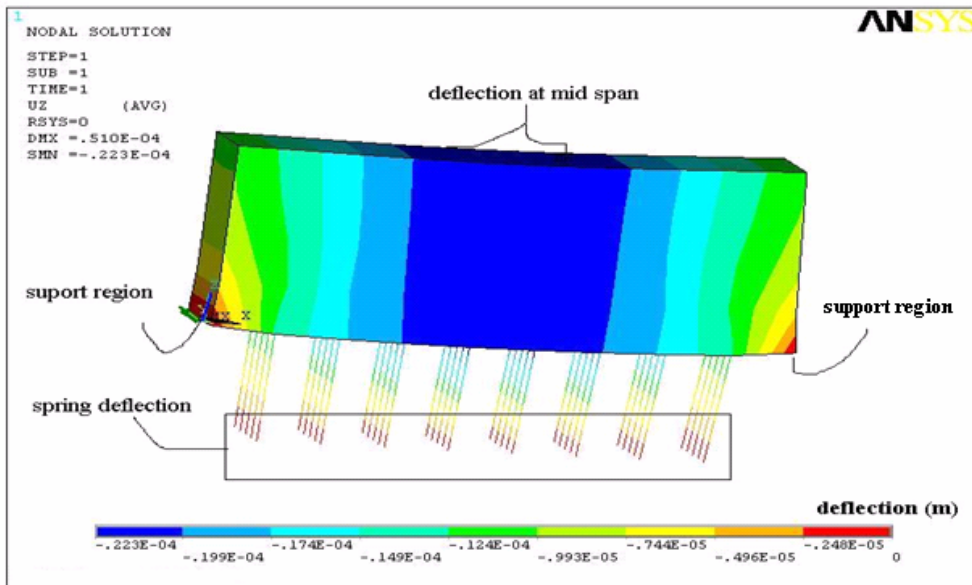


Fig. 15. Contour plot for deflection of uniformly loaded simply supported deep beam resting on Winkler foundation.

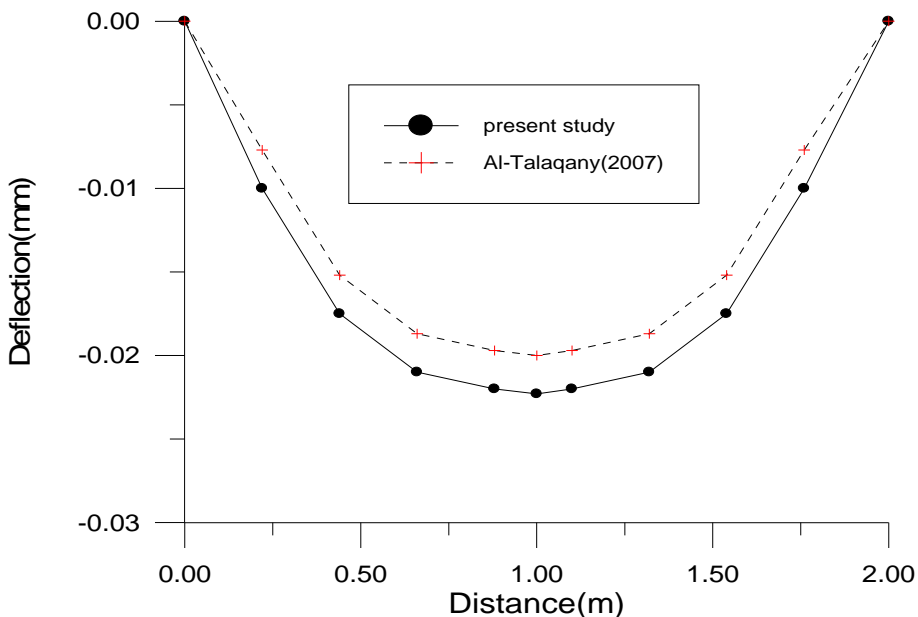


Fig. 16. Deflection curves of uniformly loaded simply supported deep beam resting on Winkler foundation.

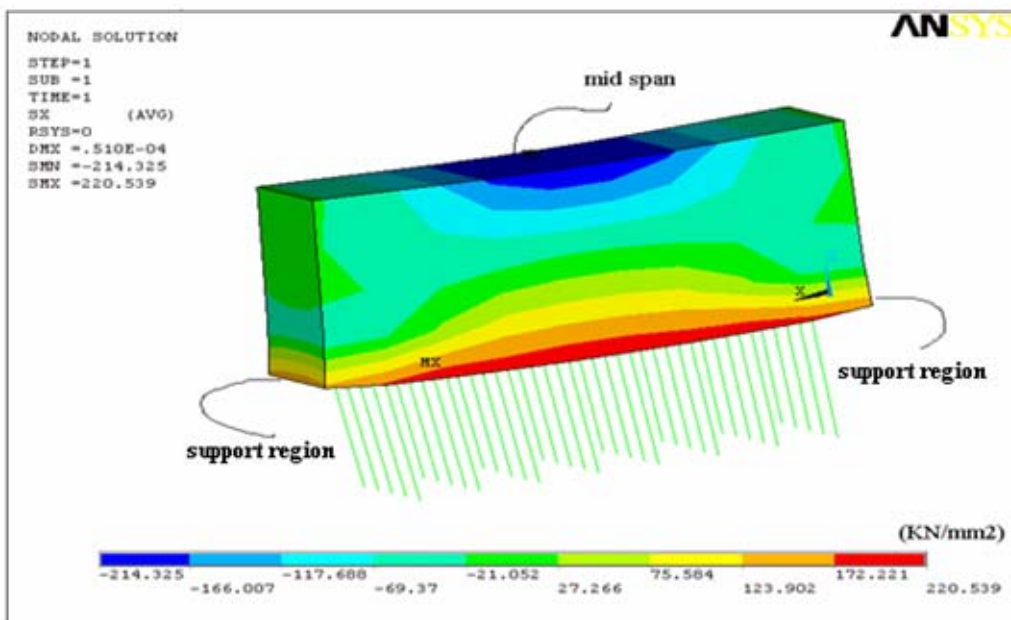


Fig. 17. Contour plot of normal stress in x-direction of uniformly loaded simply supported deep beam resting on Winkler foundation.

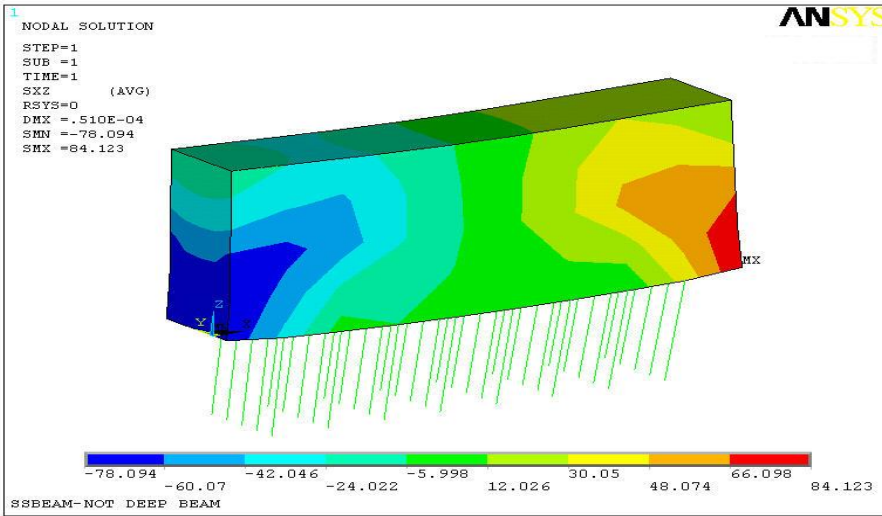


Fig. 18. Contour plot of shear stress in xz plane of uniformly loaded simply supported deep beam resting on Winkler foundation.

4.2 Free ends deep beam on nonlinear Winkler foundation with end load

A beam of ($E=25 \times 10^6 \text{ kN/m}^2$, $\nu=0.15$) and having a length of (1.8m), width ($b=0.2\text{m}$), depth ($h=0.45\text{m}$) and subjected to a concentrated load ($P=220.5 \text{ kN}$), is considered as shown in figure 19. The beam is resting on nonlinear Winkler foundation with modulus ($K_z=2000 \text{ kN/m}^3$) ($a=0.163$, $b=0.482$) and this value is obtained from plate-load test. This problem was analyzed by Hateam (2001) by using the beam-column method. In the present study, the finite-element method is used to solve this problem. The concrete beam is idealized using 11 brick elements (SOLID65) and modeled by 6 nonlinear spring elements (COMBIN39) to represent the soil nonlinear behavior as shown in figure 20. The equation of nonlinear spring is defined earlier. The present study and Hateam (2001) results of deflections are plotted as shown in figures 21 to 24. The percentage difference between the two solutions is (2.5%) which shows good agreement. The difference between large and small deflection theories are found to be very small and about (0.0012%) and can be neglected because of the effect of foundation stiffness.

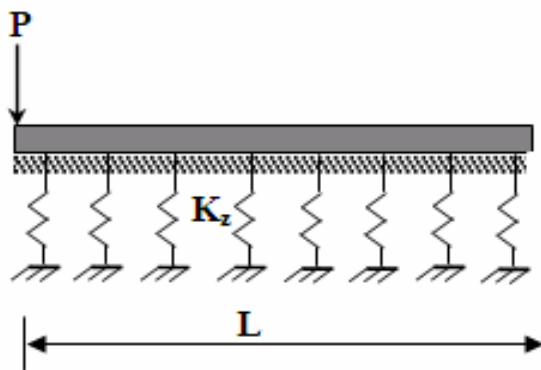


Fig. 19. End loaded free-ends deep beam resting on nonlinear Winkler foundation.

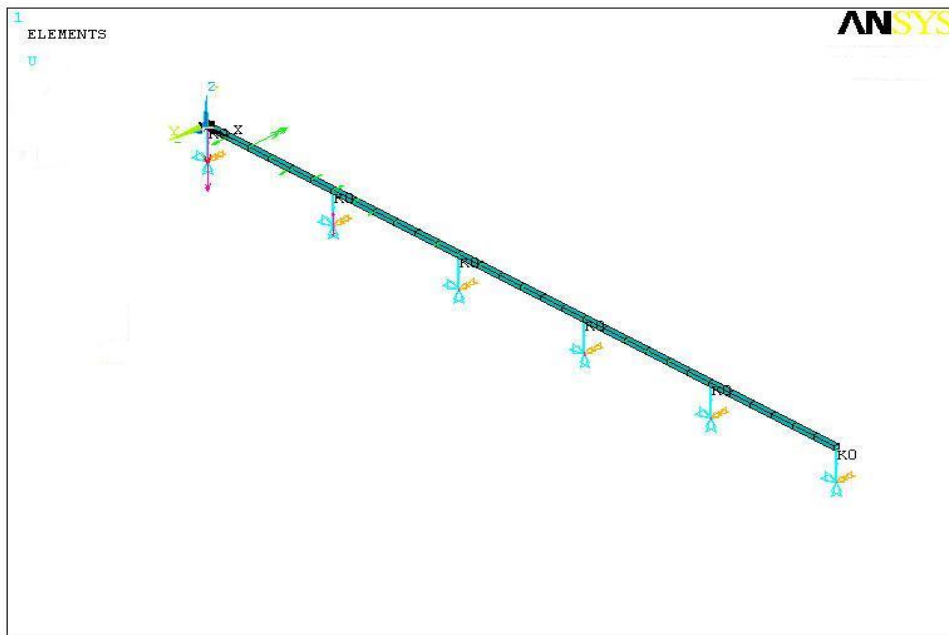


Fig. 20. Finite element mesh of end loaded free-ends deep beam resting on nonlinear Winkler foundation.

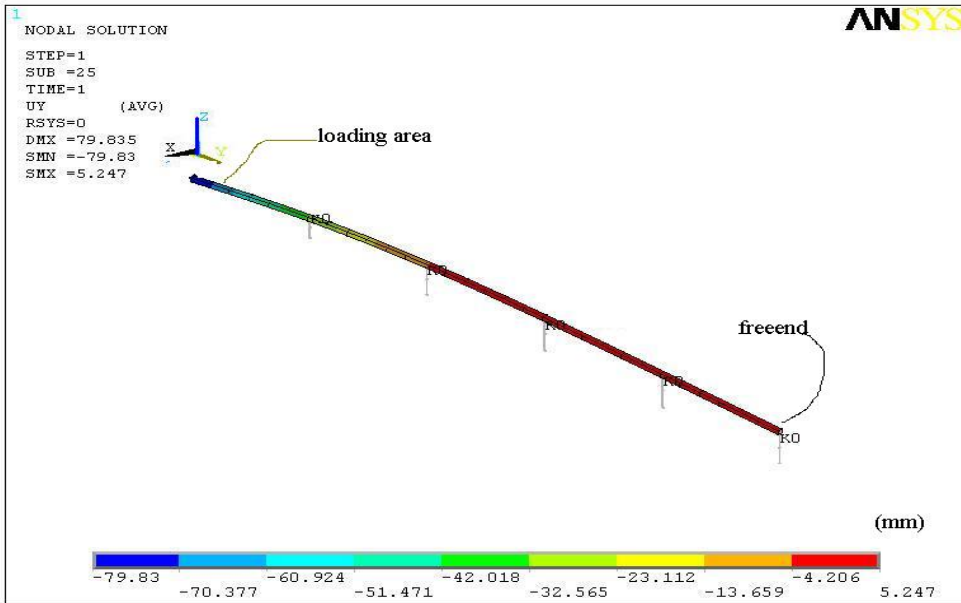


Fig. 21. Contour plot for deflection for the free-ends deep beam resting on nonlinear Winkler foundation (small deflection theory).

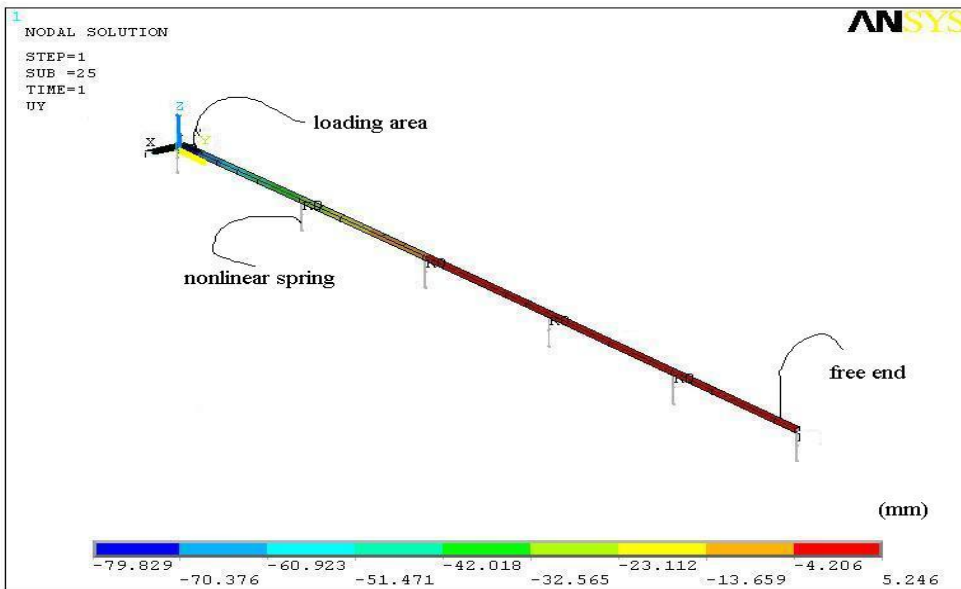


Fig. 22. Contour plot for deflection for the free-ends deep beam resting on nonlinear Winkler foundation (large deflection theory).

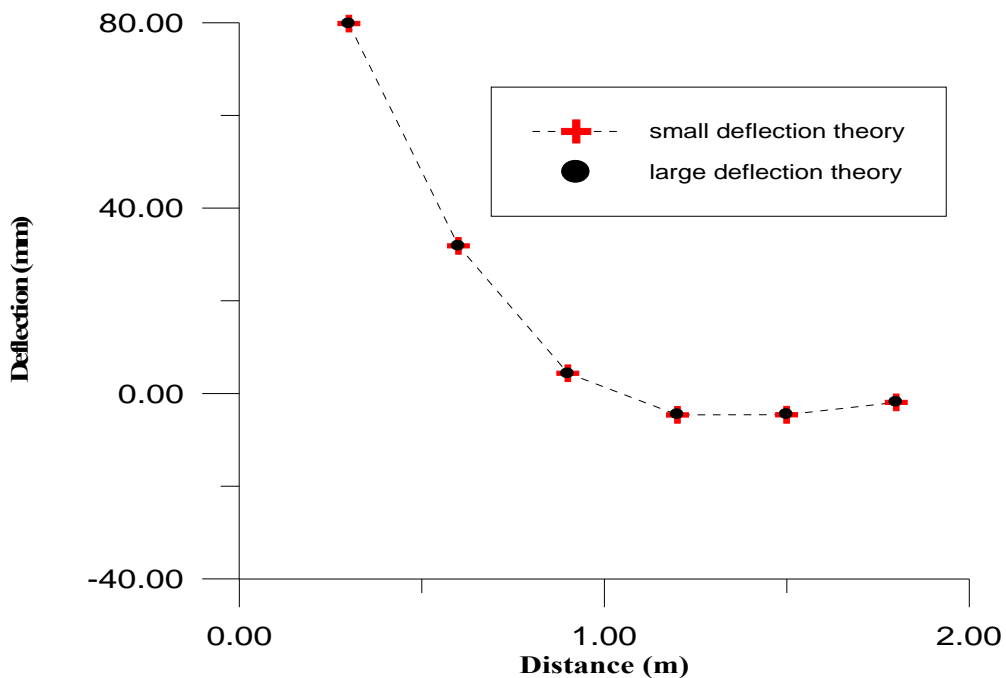


Fig. 23. Deflection curves of the free ends deep beam (small and large deflection theories) at load 220.5kN.

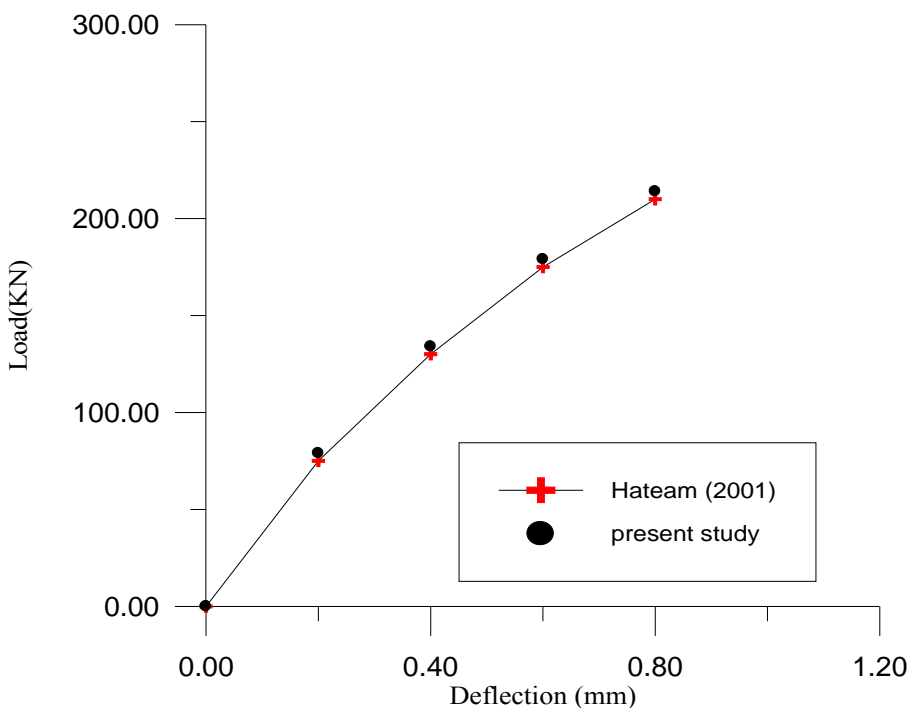


Fig. 24. Load-deflection curves for the free-ends deep beam resting on nonlinear Winkler foundation at load 220.5kN.

4.3 Parametric study

A parametric study is performed to investigate the influence of several important parameters on the behavior and strength of reinforced concrete deep beams resting on Winkler foundation and subjected to static loads.

The following important parameters are studied and discussed in this section:

- Effect of mesh size.
- Effect of subgrade.
- Effect of compressive strength.

4.3.1 Mesh size

In this section, a study has been made to investigate the effect of the mesh size on the load-deflection response of continuous reinforced concrete deep beam under concentrated load (320 kN). The beam having a length of (3.0m), width (0.12m), depth (0.625m), $f'_c=28 \text{ N/mm}^2$, $f_t=2.11 \text{ N/mm}^2$ is considered here. Mesh size effect is investigated by assigning two different meshes having 240 and 4368 elements as shown in figures 25 and figure 27. When the number of element increased, the error in calculating deflection decreased, but when we reach a specific number of mesh sizes, the effect will be small on the results. The obtained results and the load deflection curves of this investigation are shown in figure 29. It can noted that using mesh size of 4368 elements gives good agreement with the experimental load-deflection curves.

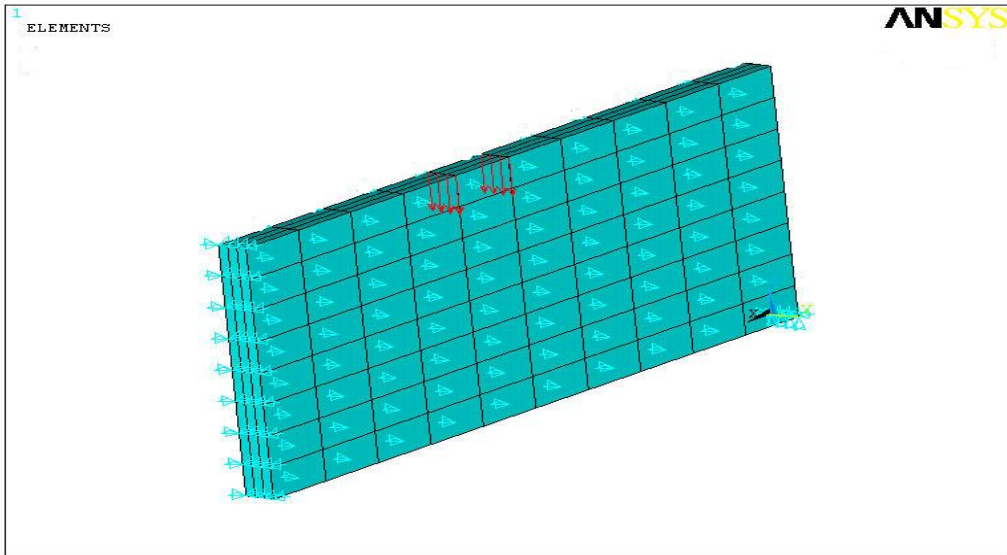


Fig. 25. Finite element mesh of simply supported reinforced concrete deep beam (240 elements mesh).

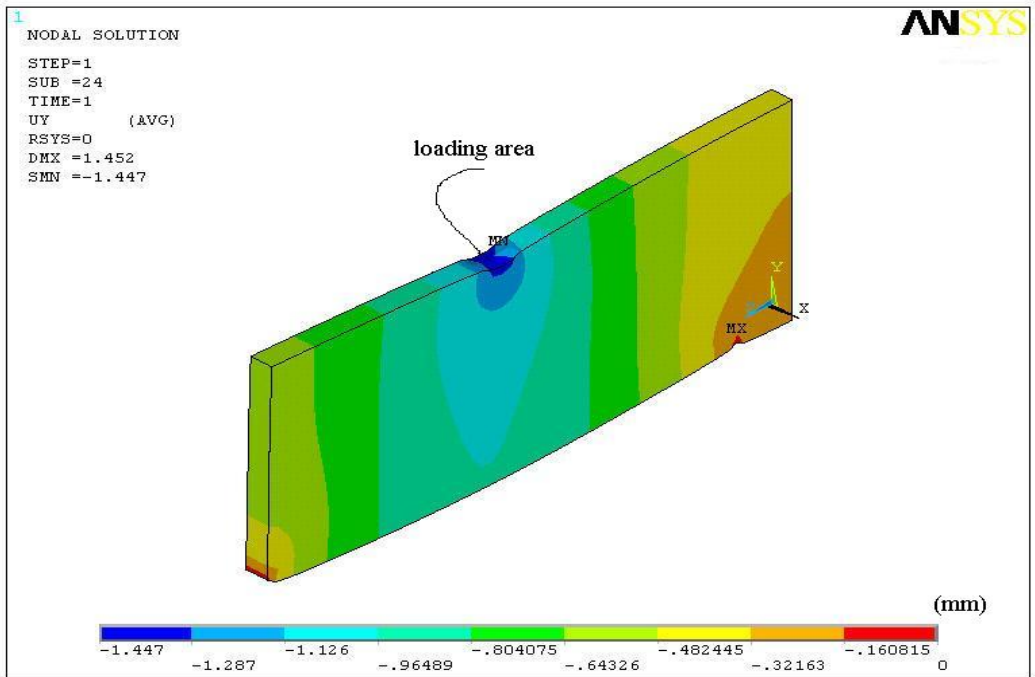


Fig. 26. Contour plot for deflection of deep beam (240 elements mesh).

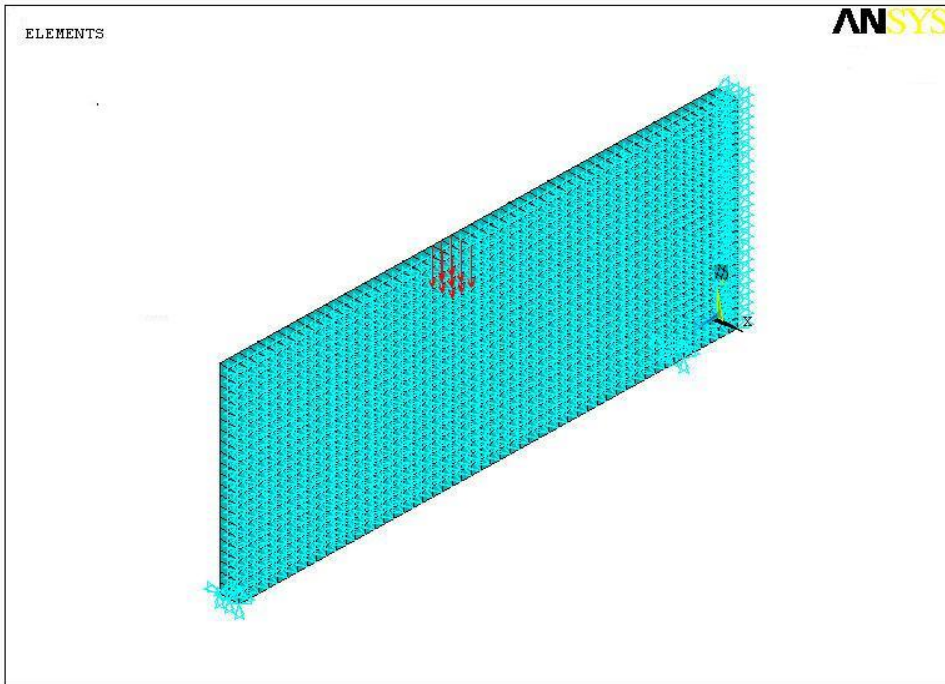


Fig. 27. Finite element mesh of simply supported reinforced concrete deep beam 3468 elements.

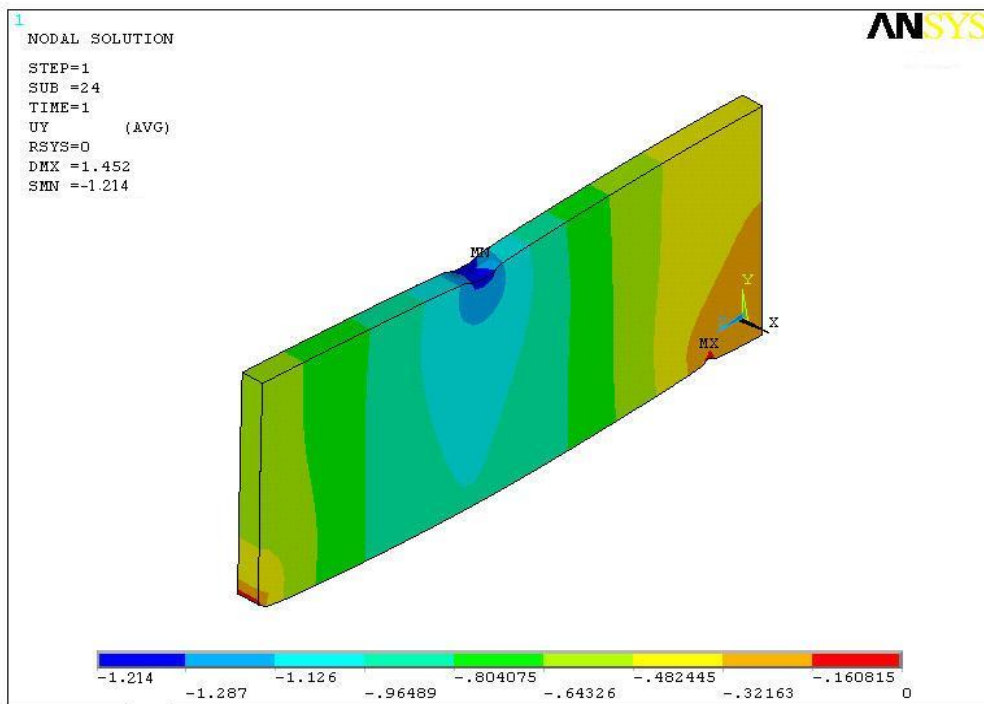


Fig. 28. Contour plot for deflection of reinforced deep beam (4368 elements mesh).

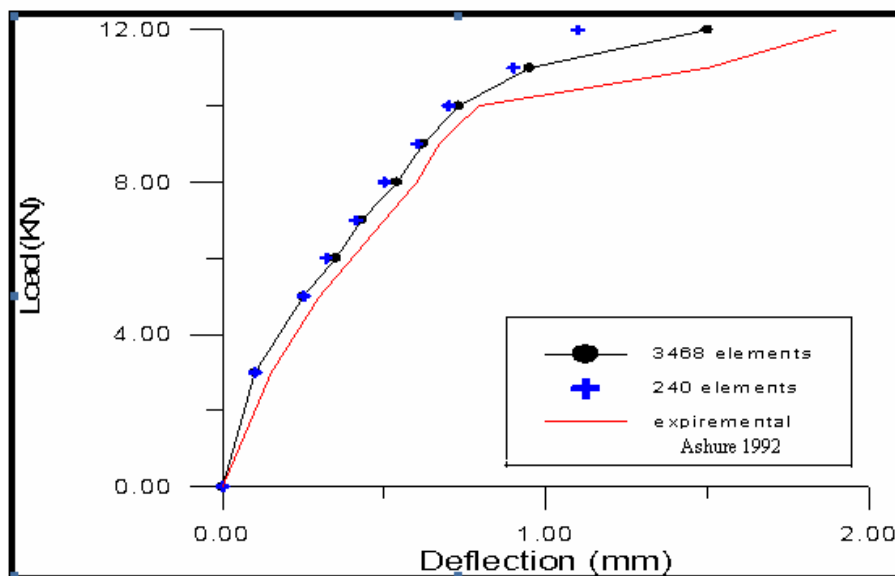


Fig. 29. Load -deflection curves of reinforced concrete deep beam.

4.3.2 Effect of subgrade

To show the effect of vertical subgrade reaction ($K_z=10000kN/m^2$) on the results, the reinforced concrete beam is idealized using 200 brick elements (SOLID65) and the steel reinforcement is assumed to be smeared throughout the elements. The foundation is modeled by 33 nonlinear spring elements (COMBIN39) as shown in figure 30. Figure 31 shows the effect of nonlinear Winkler foundation on the maximum deflection for a simply supported deep beam under a concentrated load. From this figure, the deflection will increase when the foundations modeled as a beam on nonlinear Winkler foundation, because of the ability of the model to trace the real behavior of soil and the reduced modulus of subgrade reaction which is fixed in the linear model. The maximum deflection for the simply supported deep beam under a concentrated load is increased by (2.5%). Figure 32 shows the effect of nonlinear Winkler foundation on normal stress in x-direction of a simply supported deep beam under a concentrated load. From this figure, the maximum stress will increase when the beam is on nonlinear Winkler foundation with percentage of (3.6%) because of reduced stiffness.

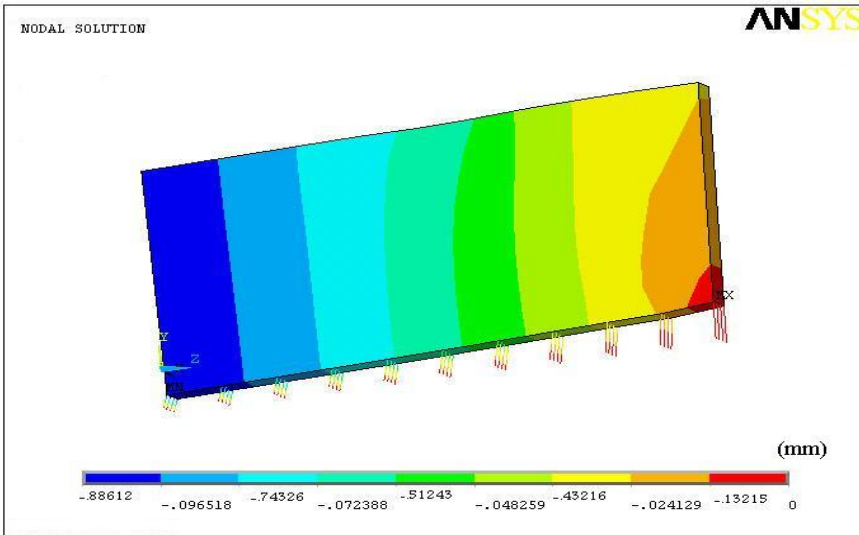


Fig. 30.Contour plot for deflection of simply supported deep beam under concentrated load on nonlinear Winkler foundation.

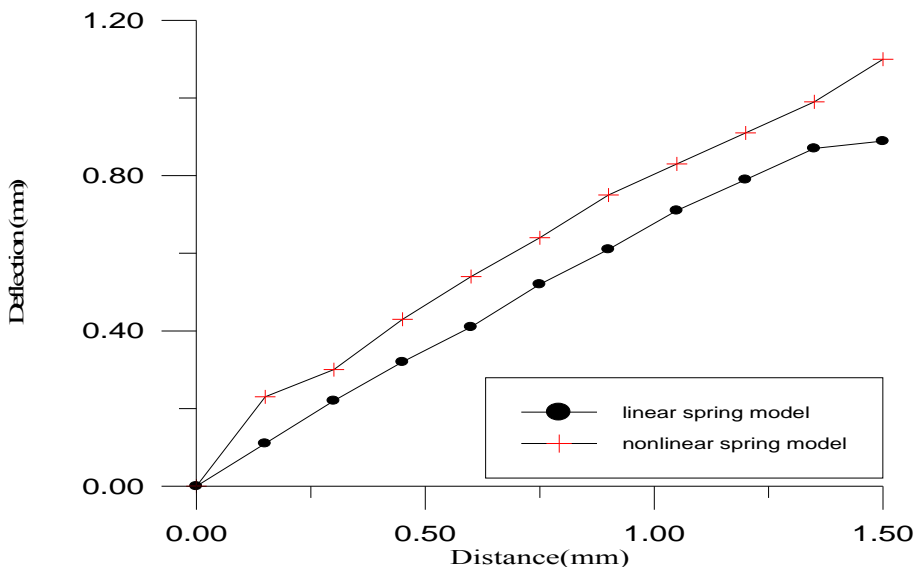


Fig. 31. Deflection curves of simply supported deep beam under concentrated load on linear and nonlinear Winkler foundation.

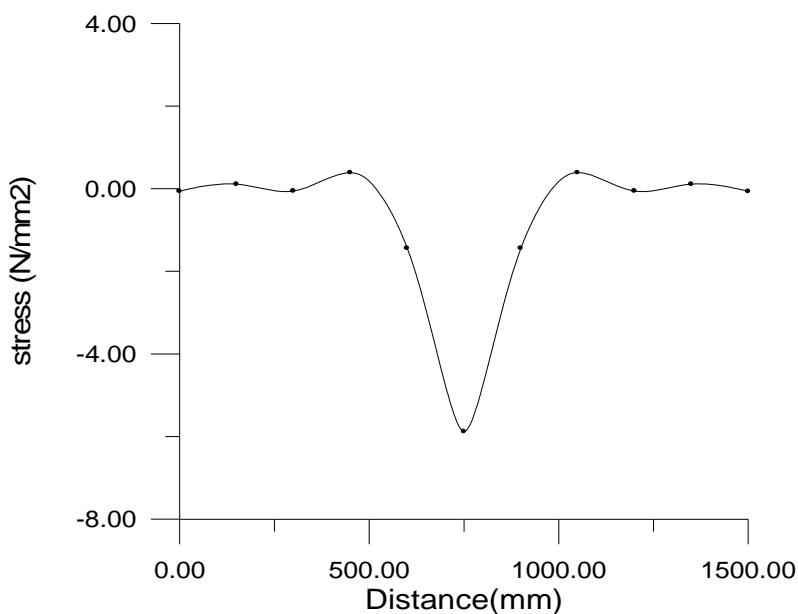


Fig. 32. Normal stress curve in x- direction of simply supported deep beam under concentrated load on nonlinear Winkler foundation

4.3.3 Effect of compressive strength

In this study, different values of the compressive strength of concrete have been used. These values were 20, and 50 N/mm². It can be noted that by increasing the compressive strength of concrete, the failure load is increased and the deflection is decreased (because of increasing in

the value of modulus of elasticity). When the concrete compressive strength increases from 20 to 50 MPa, the ultimate load is increased by 20.07% as shown in figure 33.

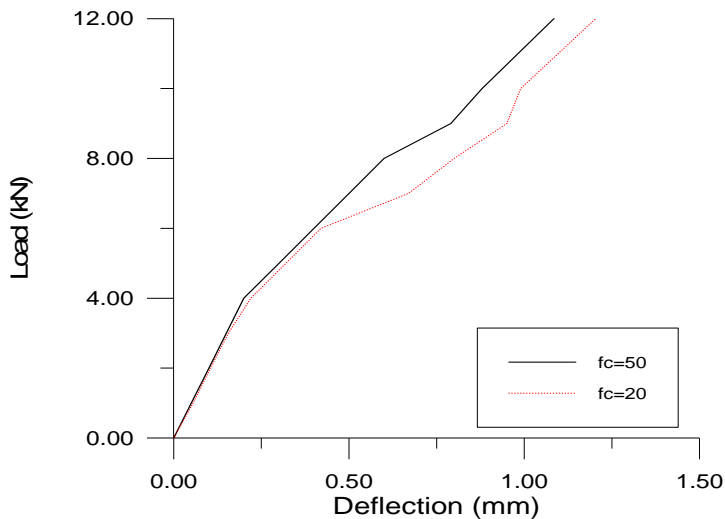


Fig. 33. Effect of the compressive Strength of concrete on the predicted load deflection response

5. Conclusions

Based on the finite element analyses carried out in this research, the following conclusions are drawn:

- Based on comparison of the computed results with the available analytical and experimental data, it is verified that the finite element method and materials models used in utilizing ANSYS computer program are reliable and accurate to predict the behavior of nonlinear geometric and nonlinear material behavior of deep beams resting on linear and nonlinear Winkler foundation.
- The ANSYS v11 program that is used in the present study shows good agreement for deflections of about (8%).
- It can be noted that by increasing the compressive strength of concrete the failure load is increased and the deflection was decreased (because of increasing the modulus of elasticity and different stress-strain curves). When the concrete compressive strength increases from 20 to 50 MPa the ultimate load is increased by 20.07%.
- The effect of large deflections on deep beams was found to be small on results in about (0.11%).
- The maximum deflection is increased by (2.5%) when the foundation is modeled as a beam on nonlinear Winkler model rather than linear Winkler model because of the cumulative deflection with load increments and reduced modulus subgrade reaction .

Извод

Анализа методом коначних елемената дубоких греда на еластичним подлогама**Dr. Adel A. Al- Azzawi¹, Aula H. Mahdy² and Omar Sh. Farhan³**

1Nahrian University, Baghdad, Iraq
dr_adel_azzawi@yahoo.com

2Nahrian University, Baghdad, Iraq
aula84@yahoo.com

3Nahrian University, Baghdad, Iraq
ommar-shamal2006@yahoo.com

Резиме

Ово истраживање се односи на материјално и геометријски нелинеарна понашања ојачаног бетона дубоких греда које се ослањају на линеарну или нелинеарну Винклерову (Winkler) подлогу. Метод коначних елемената је примењен користећи ANSYS (Release-11, 2007) компјутерски софтвер. Ојачани бетон дубоке греде је моделиран коришћењем (SOLID 65) 8-чворног тродимензионалног елемента, а тле је моделирано помоћу елемента линеарне опруге (COMBIN 14) или нелинеарне опруге (COMBIN39).

Резултати добијени у овој студији су поређени са расположивим аналитичким и експерименталним резултатима. Добијено је добро слагање са расположивим резултатима, што показује и ефикасност методе коначних елемената коришћене за моделирање овог проблема. Утврђена је мала разлика у максималном угибу према теорији малих и великих угиба. Максимални напон је увећан када се греда ослања на нелинеарну Винклерову подлогу услед смањене крутости подлоге.

Неколико значајних параметара су укључени у анализу, наиме вертикална подзидна ракција, величина мреже и компресиона јачина, да би се утврдили ефекти на понашање греде. Резултати показују да разлика у максималном угибу између линеарног и нелинеарног модела тла износи око 2.5%.

Кључне речи: Дубоке греде, коначни елементи, нелинеарне еластичне подлоге**References**

- ACI Committee 318 (2008). Building Code Requirements for Structural Concrete and Commentary. (ACI 318M-08), American Concrete Institute.
- Al-Azzawi A. A. and Al-Ani M. A. (2004). Finite difference analysis of beams on Winkler foundations", Engineering and Technology Journal, University of Technology, Baghdad, Iraq, **23**, No. 10, 578-592.
- Al-Hachmi E. K. (1997). Large Displacement Analysis of Structures with Applications to Piles and Submarine Pipelines. Ph.D., Thesis, University of Technology, Baghdad, Iraq.

- Al-Musawi A. N. (2005). *Three Dimensional Finite Element Analysis of Beams on Elastic Foundations*. M.Sc. Thesis, Faculty of Engineering, Nahrain University, Baghdad, Iraq.
- Al-Shraify B. I. (2005). *Nonlinear Finite Element Analysis of Continuous Deep Beam on Elastic Foundation*. M.Sc. Thesis, Faculty of Engineering, Nahrain University, Baghdad, Iraq.
- Al-Talaqany D. M. (2007). *Large Deflection Deep Beams on Elastic Foundations*. M.Sc. Thesis, Faculty of Engineering, Nahrain University, Baghdad, Iraq.
- Andrejev H. (2008). Discussion to closed-form solution for reinforced Timoshenko beam on elastic foundation. *Journal of Engineering Mechanics*, American Society of Civil Engineers, December, 1317-1340.
- Aristizabal-Ochoa J. D. (2001). Nonlinear large deflection-small strain elastic analysis of beam-column with semi-rigid connections. *Journal of Structural Engineering*, American Society of Civil Engineers, **127**, No. 1, January, 92-96.
- Ashure A. F. (1992). Test of reinforced concrete continuous deep beams. *ACI Structural Journal*, **94**, No.1, January-February, 3-12.
- Chen C. N. (1998). Solution of beam on elastic foundation by DQUM. *Journal of Engineering Mechanics*, December, 1381-1384.
- Chen W.F. (1982). *Plasticity in Reinforced Concrete*. Mc Graw – Hill Book Company.
- Collins M. P. and Mitchell D. (1991). *Prestressed Concrete Structures*. Prentice Hall, Engle Wood, New Jersey.
- Guo Y. J. and Weitsman Y. J. (2002). Solution method for beams on nonuniform elastic foundations. *Journal of Engineering Mechanics*, American Society of Civil Engineers, **128**, No. 5, May, 592-594.
- Hateam K. K. (2001). Large Displacement Elastic Stability Analysis of Plane Structures under Static Load and Resting on Nonlinear Winkler Foundation. *Engineering and Technology Journal*, University of Technology, Baghdad, Iraq .
- Jamal A. (1997). *Large Displacement Elastic Stability Analysis of Gusseted Frames*. M.Sc. Thesis, University of Technology, Baghdad, Iraq.
- Lazem A. N. (2003). Large Displacement Elastic Stability Analysis of Elastic Framed Structures Resting on Elastic Foundation. M.Sc. Thesis, University of Technology, Baghdad, Iraq.
- Mahmoud A. K. D. (2001). Nonlinear Finite Element Analysis of Reinforced Concrete Members under Long-Term Loading. Ph.D. Thesis University of Baghdad, Baghdad, Iraq.
- Onu G. (2000). Shear effect in beam finite element on two- parameter elastic foundation. *Journal of Engineering Mechanics*, September, 1104-1107.
- Yin J. H. (2000-a). Comparative modeling study of reinforced beam on elastic foundation. *Journal of Engineering Mechanics*, American Society of Civil Engineers, March, 265-271.
- Yin J. H. (2000-b). Closed-Form solution for reinforced Timoshenko beam on elastic foundation. *Journal of Engineering Mechanics*, American Society of Civil Engineers, **126**, No. 8, August, 868-874.